Rev.Adv.Mater.Sci. 6 (2004) 162-168

MODELING THE ORGANIC-INORGANIC INTERFACIAL NANOASPERITIES IN A MODEL BIO-NANOCOMPOSITE, NACRE

Dinesh R. Katti, Shashindra Man Pradhan and Kalpana S. Katti

Department of Civil Engineering, North Dakota State University, Fargo ND 58105, USA

Received: February 25, 2004

Abstract. Nacre, the inner iridescent layer of several mollusk seashells is a model nanocomposite with exceptional mechanical properties, that is composed of layers of organic (proteins and polysaccharides) and inorganic (aragonite). A 3D finite element model of nacre was constructed that incorporates the nanometer sized asperities at the organic-inorganic interfaces to evaluate their role on mechanical response of nacre. Simulations were performed on a 3×3×1 block model of nacre to evaluate the influence of nano-asperities on overall mechanical response of nacre. A small increase in elastic modulus results from the presence of asperities. In inelastic regime, the effect of nano-asperities on yield stress was marginal, and the strain-hardening slope was seen to decrease upon introduction of nano-asperities. In addition, the nano-asperities resulted in increase in the magnitude of plastic strains after the yield. These series of simulations suggest that nano-asperities have marginal effect on the overall mechanical response of nacre. Although our simulations show that the presence of nano-asperities only marginally improves the mechanical properties, their presence in the biological nanocomposite may provide large surface area for the organic to attach and interact with the inorganic. The organic matrix in nacre has previously been shown to be a material with exceptional properties. The nano-asperities could also provide confinement of biopolymers (proteins and polysaccharides) resulting in enhanced mechanical properties of the organic layer.

1. INTRODUCTION

Nacre, the iridescent inner layer of mollusk shells is a model biocomposite. It is made of a hierarchical morphology characteristic of structural materials of nature such as bone, teeth and seashells. The structure of nacre has been investigated extensively in literature [1-7]. Nacre is composed of highly organized polygonal shaped aragonitic calcium carbonate platelet layers of thickness of 0.2-0.5 μm separated by 20-50 nm layers of biopolymers composed mainly of proteins and polysaccharides [5,6,8,9]. This structure is often called as a 'brick and mortar' and is responsible for the high strength and fracture toughness of nacre. Mechanical testing illustrates that nacreous structure is strongest in tension, compression, and bending compared to other shell structures. It exhibits a work of fracture three orders of magnitude higher than monolithic ceramics [10,11] and 3000 times that of pure aragonite [12]. Due to these exceptional properties, this material is extensively studied as an inspiration for design of novel high strength composites. The composition of interface and interactions within it when the load is applied is the least understood aspect of nacre. The interface is complicated because there is no distinct region of separation between inorganic and organic regimes; also the composition of the interface, and the molecular-scale interactions between the constituents (organic and inorganic) when stress is applied is not known.

Corresponding author: Dinesh R. Katti, e-mail: Dinesh.Katti@ndsu.nodak.edu

Further, mineralized bridge like structures were reported at the center of aragonite bricks by various researchers using electron microscopy [13-16]. These mineral bridges are a number of small mineral structures that pervade through the organic and connect aragonite brick surfaces at different layers. Recently a number of pores on the organic matrix of nacre were observed [17] which were proposed to be mineral bridges. In addition these mineral bridges were directly observed in organic matrix layers of nacre of *Haliotis Iris* species with a transmission electron microscope (TEM). The mineral bridges were approximately circular with a diameter of 25~34 nm and the height equal to thickness of organic layer. The density of mineral bridges on the surface of aragonite platelet are found to be approximately 91~116 μm^{-2}.

In our previous work, simulations have demonstrated the application of Finite Element Method as a powerful tool for modeling mechanical response of nacre [18-20]. The simulation results have led to some important findings that help explain elastic and inelastic mechanical properties of nacre. The linear simulations at low loads (2 MPa) which lie well within elastic regime of nacre predicted the necessity of high elastic modulus of organic (~15 Gpa). Following the prediction of high value of modulus and yield stress of organic, Katti *et al.* [19] investigated the role of mineral bridge contacts on mechanical response of nacre. In this model the hexagonal prismatic mineral bridge contact with 25 nm long sides was provided at the center of each brick, and each brick was rotated 5° relative to each other in direction normal to plane face of brick. Simulations were also done without presence of any mineral contacts. The results showed that the elastic response of nacre is only marginally influenced by presence of contacts irrespective of how high the value of elastic modulus of contact is chosen [20]. Further, the influence of contacts on yield behavior of nacre was also investigated. It was shown that the contact regions yield long before nacre starts to yield at ~ 60 MPa [19]. In addition prior work also showed that the high yield strength of organic is necessary to obtain experimentally observed yield strength of nacre. Since these simulations were carried out considering aragonite phase to be perfectly elastic, authors also pointed out the possibility of aragonite being elastoplastic in nature. The elastoplastic behavior of inorganic is believed by authors to underscore the possibility of very high yield strength of organic given its composite nature.

Recently, mineral island-like structures were observed using atomic force microscopy (AFM) and scanning electron microscopy (SEM) [21-22]. Their observation of red abalone (*Haliotis rufescens*) nacre specimen revealed nanoscale mineral islands (asperities) that were about 30-100 nm in diameter, 10 nm in amplitude, and separated by 60-120 nm. In this work the organic-inorganic interface is modeled in a nano-meso scale and embedded into a micro-scale model of nacre. This work deals with finite element modeling of nanoscale roughness (asperities) at the organic-inorganic interfaces and its effect on the mechanical response of nacre.

2. DESIGN OF MODELS USED FOR SIMULATION

The 3D FEM model is composed of layers of hexagonal aragonite bricks and organic matrix arranged according to a brick and mortar architecture. The micro nano-architecture of model resembles that of columnar nacre. The consecutive blocks of nacre at different layers are rotated by 5 degrees with respect to each other. The nano-asperities are scattered on the surfaces of aragonite brick protruding towards organic matrix. The dimension of aragonite brick is 2500 nm in width and 250 nm in height and the organic matrix sandwiched between bricks is 20 nm thick. Nano-asperities are chosen to be 50 nm wide and 10 nm tall with 50 nm distance of separation among themselves. A magnified isometric view of an edge of model showing nano-asperities on surface of aragonite bricks is shown in Fig. 1.

The FEM model was constructed using a preprocessor and post processor MENTAT™ (MSC Marc Corp) on a silicon graphics workstation. This model follows the basic framework similar to our previous model [20], but incorporates nano-asperities on the surface of aragonite so that their effect on the overall mechanical response of nacre can be evaluated. Since the nano-asperities are relatively small compared to aragonite and numerous, model building posed challenges for accurately modeling the nano-mesostructure of nacre using available computational infrastructure. The simulations were conducted on National Center for Supercomputing Applications SGI ORIGIN 2000 and IBM P690 Supercomputer System. The method outlined next was used to build the model to study the role of nano-asperities on elastic and inelastic deformation of nacre.

This model is based on the 'brick and mortar' micro-nano-architecture of nacre with parameters as shown in Table 1. The model comprises of layers of

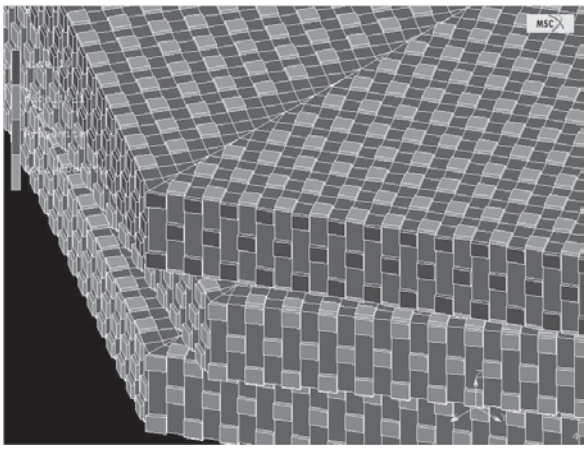

Fig. 1. Magnified isometric view of an edge of model showing nano-asperities on surface of aragonite bricks.

hexagonal aragonite platelets with asperities embedded all over its surface, and the organic sandwiched between them. The aragonite bricks and the asperities were constructed from eight-noded isoparametric elements. The distribution of nano-asperities on the top and bottom surface of hexagonal aragonite bricks was assumed to have 6-fold rotational symmetry. The nano-asperities were spread uniformly on the surface of aragonite keeping a distance of separation 50 nanometers between them.

The model is built using a triangular element, obtained by merging two top-nodes of a quadrilateral element. The triangle was equilateral in shape with sides 2.5 μm long. This triangular plate was expanded along z-direction by 250 nm to obtain a prismatic element that comprises one sixth of an aragonite brick. The prism was filled with eight-noded brick elements so that the nodes become available on its surface for appending nano-asperities. This was carried out by subdividing the triangular prism in *xy*-plane to fill it with number of quadrilateral elements. Material property of aragonite was assigned to all the elements in the prism.

Similarly, the construction of organic layer started with a triangular plate filled with quadrilateral elements 50 nm wide. The alternate quadrilateral elements were assigned properties of inorganic and organic. The elements with properties of organic were then subdivided along *y*-axis into two divisions. This triangular plate was duplicated in a *xy*-plane by rotating 5 degrees about the top vertex. These two triangular plates, rotated with respect to each other, were connected to each other by moving and merging nodes located in an organic zone. Moving of nodes attached to an element assigned with property of inorganic was avoided to ensure that there is no rigid contact between asperities. After connection between these two triangular plates has been established, these plates were expanded in opposite *z*-directions to obtain a 3D brick elements.

Our 3D model incorporates improvements in transitioning of mesh in the organic and inorganic interface. The difficulty in providing a good transitioning of mesh originates from the inability to incorporate greater number of elements in the model. Increase in number of elements in the mesh transition zone (at interface between inorganic and organic) results in a larger model that far exceeds the existing computational resource. This difficulty is overcome by attaching organic layers to the sides of inorganic brick by utilizing 'glued contact' feature of MSC Marc software. Glued contact is a special type of friction model, for defining contact between to bodies, which can be used to join two dissimilar meshes. The layers containing nano-asperities embedded in the matrix of organic were then attached to those faces of prism that correspond to outer surface of aragonite. A tower consisting of three triangular bricks was formed. The side organic with the asperities embedded were also attached to the triangular brick that corresponds to outer face of aragonite. Upon five-fold duplication of this tower (rotating 60 degrees during each duplication, about central axis of aragonite), the columnar brick tower with asperities attached to its surface and laminated with organic is obtained.

Table 1. Comparison of stress/strain ratio in presence and absence of nano-asperities.

Model Type	Elastic modulus used in simulation		Modulus (GPa)		
	Inorganic	Organic	Max area	Av. area	Min area
Without Nano-asperities	99.5 GPa	20 GPa	52.46	69.95	104.93
With Nano-asperities	99.5 GPa	20 GPa	54.83	73.11	109.67

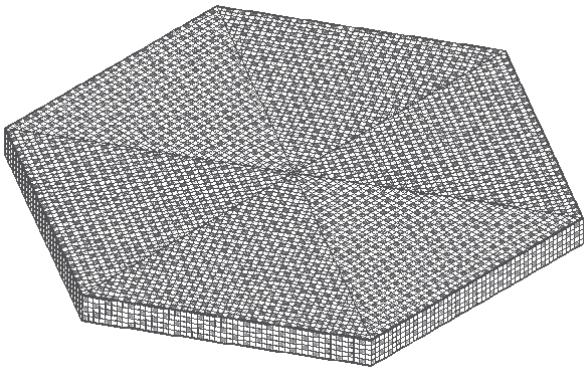

Fig. 2. Nano-asperities on the surface of aragonite represented by dark spots on surface and organic represented by faint spots.

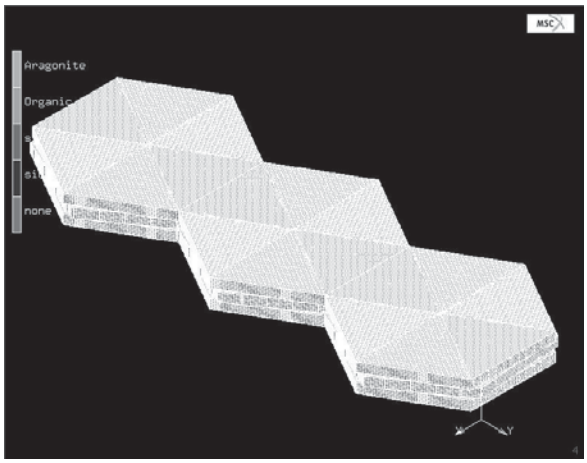

Fig. 3. A 3×3×1 model of nacre showing nano-asperities.

The duplicate nodes formed due to overlapping of nodes are later swept away. This columnar tower consisting of three hexagonal bricks in a stack is duplicated and translated along *y*-axis two times by 4350. 127 nanometers to obtain a 3×3 model. Nano-asperities on the surface of aragonite are shown in Fig. 2. In this case, the connection between the organic layers on the edges of brick is established through predetermined location of nodes.

The model size is maintained at 3×3×1. The total number of 3D elements used were 188,352. Fig. 3 shows the complete model. For conducting simulated tensile and compressive tests, uniform load was applied on edges of aragonite in the direction parallel to the platelet; the organic layer was stripped at the faces where boundary conditions are applied.

3. SIMULATION DETAILS

3.1. Simulations in Elastic Regime

The simulated tensile and compressive tests were performed separately on 3×3×1 aragonite-brick models with and without nano-asperities. The tensile and compression tests were performed at an applied load of 2 MPa uniformly distributed across the width of aragonite brick in a single load increment. The applied load vs. strain observed is compared to understand response in presence and absence of nano-asperities.

3.2. Simulations in Inelastic Regime

As with simulation in elastic regime the 3D model composed of 3×3×1 aragonite was used in this analysis. Both the cases with and without nano-asperities were analyzed. The yield stress (σ_y) of inorganic layer was fixed at 30 MPa, which is a typical value for geological aragonite, whereas the yield stress (σ_y) of organic phase was varied from $40 \cdot 10^{-6}$ N/μm^2 to $160 \cdot 10^{-6}$ N/μm^2. The yield strength of aragonite available as a geological deposit had been used for this simulation as a good experimental data for aragonite of biological origin in not available. Our studies showed that the yield stress of organic has very little effect on the bulk yield stress of nacre. The modified Newton-Raphson integration scheme was used for numerical integration. Further, we used Von Mises yield criterion and an isotropic work hardening rule. The tensile and compressive load path of 0 to $22 \cdot 10^{-6}$ N/μm^2 (22 MPa) uniformly distributed across the full width of aragonite brick was applied to the model in increments of $2 \cdot 10^{-6}$ N/μm^2 (2 MPa) and 2.5 N/μm^2 (2.5 MPa) for varying yield stress of organic phase. Yield stress of organic phase was maintained at $40 \cdot 10^{-6}$ N/μm^2, $80 \cdot 10^{-6}$ N/μm^2, and $160 \cdot 10^{-6}$ N/μm^2. For each value of yield stress of organic phase, stress-strain response of nacre in plotted for both the cases of with and without nano-asperities.

4. RESULTS

In the present work the role of asperities on the response in the elastic regime, and yield stress and strain hardening slope (*P*) in the inelastic regime are investigated. Since one row of blocks were used in the simulations, which results in a bar of non uniform width, a term modulus in used to define the slope of applied stress vs. strain response.

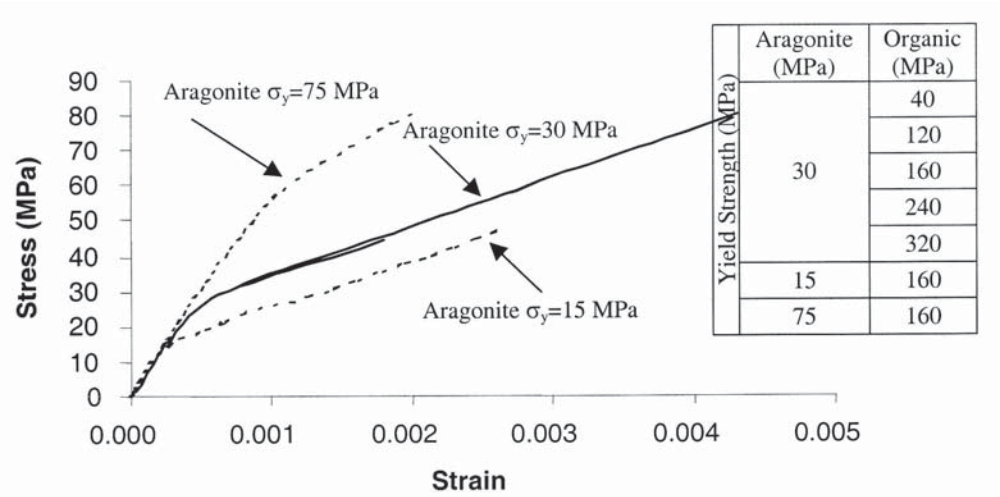

Yield Strength (MPa)	Aragonite (MPa)	Organic (MPa)
	30	40
		120
		160
		240
		320
	15	160
	75	160

Fig. 4. Simulation results of 3×3×3 model without nano-asperities for various values of yield strength of organic and inorganic showing influence on bulk yield stress of nacre. The upper and lower dotted curves correspond to aragonite yield stress of 75 MPa and 15 MPa respectively, and the continuous line curves represent 30 MPa.

Elastic response of this model in the presence and absence of nano-asperities is presented in Table 1. It is worth noting at this point that our model constitutes a chain of three columns of aragonite bricks placed side to side. Therefore when the tensile load is applied along the length of chain, the calculation of equivalent applied stress is complicated by the varying cross sectional area of our model. This effect is minimized in a bigger model, which has sufficient number of aragonite bricks in *xy*-plane. Because of this difficulty in finding exact value of Young's modulus from the existing model, only the lower and upper bounds of elastic modulus are presented in Table 1. The lower bound of elastic modulus corresponds to the stress approximation assuming load applied across entire width of aragonite brick- 'maximum area approximation'. The upper bound of elastic modulus corresponds to the stress approximation assuming load applied across the width of single edge of aragonite brick- 'minimum area approximation'. In addition to this, the average modulus corresponding to equivalent width of bar, which has a volume as our model, is also presented. It is seen from the table that the values of upper bound modulus (minimum area approximation) are larger than the Young modulus of constituents (i.e. inorganic and organic) and therefore unrealistic. This is due to unrealistically high value of applied stress obtained from 'minimum area approximation' of stress. However, since the model geometries for both cases, with and without nano-asperities are the same, stresses computed by either of the methods (as long as it is the same method) can be used to evaluate the effect of nano-asperities.

It is seen from the results of simulations conducted in elastic regime that the elastic modulus in the presence and absence of asperity are 73.11 GPa and 69.95 GPa respectively (average area approximation). The rise in modulus in presence of nano-asperities is about 4.5%. In the current model the nano-asperities constitute about 31% of the volume of organic matrix. Therefore this increase in modulus can be attributed to two reasons. Firstly, the increased modulus is due to the displaced volume of organic matrix by nano-asperities that has an elastic modulus five times larger then organic. Second contributor to increased modulus is the structural stiffness provided by resistance of nano-asperities to bending or twisting deformations.

In inelastic regime no significant difference was observed in the yield stress in presence and absence of nano-asperities, though the yield stress seems to be marginally improved by nano-asperities. After yielding, the presence of nano-asperities resulted in greater plastic strain than without them. This reduction in strain hardening due to presence of nano-asperities can be observed in Figs. 5-7. These plots present the inelastic response of model when the yield stress of organic is 40 MPa, 80 MPa, 120 MPa, and 160 MPa.

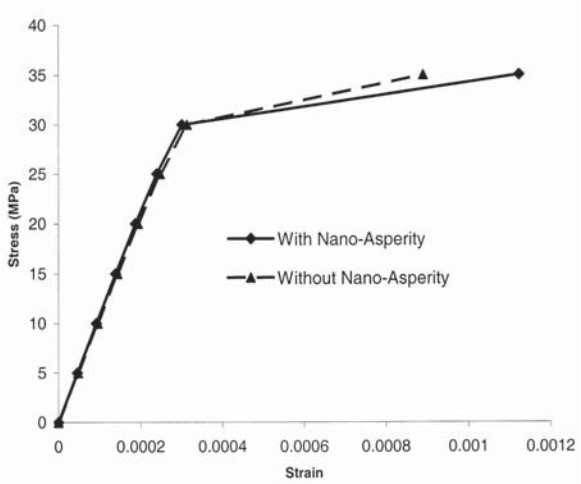

Fig. 5. Stress-strain response in presence and absence of asperities for yield stress of aragonite and organic 30 MPa and 40MPa respectively.

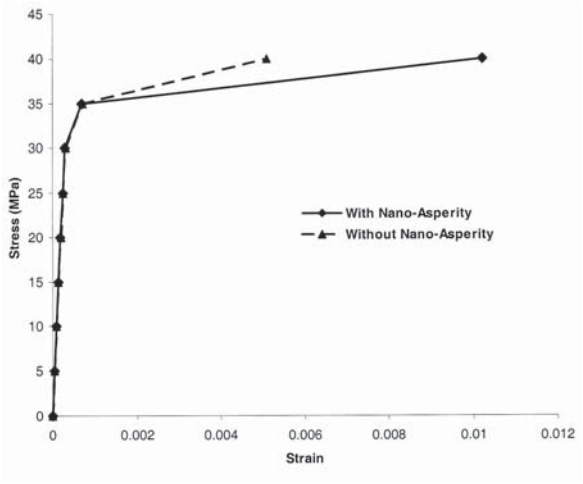

Fig. 6. Stress-strain response in presence and absence of asperities for yield stress of aragonite and organic 30 MPa and 80MPa respectively.

Moreover, the observation of these stress-strain plots at various yield stress of organic reveals almost the same value of yield stress. This is a further verification of our previous suggestion that the yield stress of nacre is controlled by the yield stress of inorganic brick. This result has an important implication on the yield stress of nacre because it entails the yield stress of aragonite bricks to be at least as high as the actual yield stress of nacre. This conclusion can be verified once yield stress of aragonite brick is obtained from nanoindentation experiments.

It is worth recalling at this point, the result of our previous work [20] that the yield strength of organic must be higher than the yield stress of inorganic. The confirmation of this result through experimentation has an important bearing on the impact of nano-asperities on the inelastic response of nacre as entailed by the results presented. The stress-strain plots presented above indicate to us that there is a relative softening when asperities are introduced compared to without them. This might not have been the case if the yield stress of nano-asperities were greater than the yield stress of organic matrix. Hence is suggested that the observed lower strain-hardening in presence of asperities is a result of lower yield stress of inorganic compared to organic. Furthermore in an inelastic zone the adjacent asperities protruding towards each other from opposite brick surfaces were seen to deform, which is an evidence of interaction between nano-asperities.

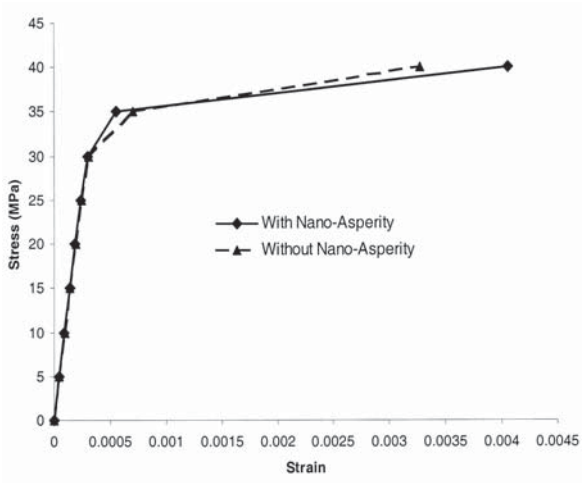

Fig. 7. Stress-strain response in presence and absence of asperities for yield stress of aragonite and organic 30 MPa and 120MPa respectively.

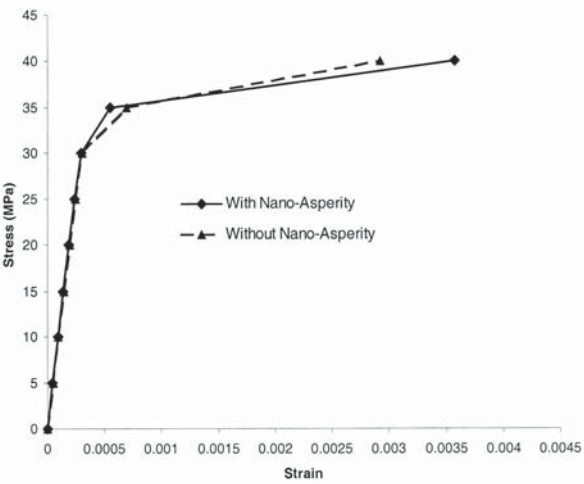

Fig. 8. Stress-strain response in presence and absence of asperities for yield stress of aragonite and organic 30 MPa and 160MPa respectively.

5. CONCLUSIONS

Simulations were performed on a 3×3×1 block model of nacre to evaluate the influence of nano-asperities on overall mechanical response of nacre. The presence of asperities resulted in a small increase in elastic modulus, part of which results from increased aragonite volume of nano-asperities and part from the structural effect of the nano-asperities. In inelastic regime, the impact on yield stress was marginal and the strain-hardening slope was seen to decrease upon introduction of nano-asperities. The magnitude of plastic strains after the yield was higher for nacre with asperities than without asperities. These series of simulations suggest that nano-asperities have marginal effect on the overall mechanical response of nacre. Although our simulations show that the presence of nano-asperities only marginally improves the mechanical properties, their presence in the biological nanocomposite may provide large surface area for the organic to attach and interact with the inorganic. The nano-asperities could also provide confinement of biopolymers (proteins and polysaccharides). The organic matrix in nacre has previously been shown to be a material with exceptional properties. The molecular nature of the protein-aragonite interfaces is clear an important issue that will further help understand the complex mechanical response of nacre, which is a subject of subsequent work [23].

ACKNOWLEDGEMENTS

The authors acknowledge support from National Science Foundation (project # 0115928). The cognizant program officer is Dr. K. Chong. The authors would like to acknowledge the National Center for Super Computing Applications (NCSA) for access to their supercomputer systems.

REFERENCES

[1] O. B. K. Boggild // *Dan. Vidensk. Selsk. Skr. Naturvidensk. Math. Afd.* **9** (1930) 233.
[2] J.D.Taylor, W.J. Kennedy and A. Hall // *Bulletin of the British Museum (Natural History), Zoology supplement* **3** (1969) 125.
[3] H. K. Erben // *Biomineralisation Forschungsberichte* **4 (**1972) 15.
[4] J.D. Taylor and M. Layman // *Palaeontology* **15** (1972) 73.
[5] J.D. Currey // *Proceedings of the Royal Society of London, Series B.* **196** (1977) 443.
[6] J.D. Currey, In: *The Mechanical Properties of Biological Materials*, ed. by J. F. V. Vincent and J. D. Currey (Cambridge University Press, London, 1980) p. 75.
[7] M. Sarikaya and I. A. Aksay // *Biopolymers* **1** (1992) 26.
[8] M. Yasrebi, G.H. Kim, K.E. Gunnison, D.L. Milius, M. Sarikaya and I.A. Aksay // *Mat. Res. Soc. Proc* **180** (1990) 625.
[9] M. Sarikaya, K.E. Gunnison, M. Yasrebi, D.L. Milius and I.A. Aksay // *Mat. Res. Soc. Proc* **180** (1990) 109.
[10] A.P. Jackson, J.F.V. Vincent and R.M. Turner // *Proc. R. Soc. London, Ser. B* **234** (1988) 415.
[11] J.D. Currey // *Proc. R. Soc. London, Ser. B* **196** (1977) 443.
[12] A.P. Jackson, J.F.V. Vincent and R.M. Turner // *J. Mater. Sci.* **25** (1990) 3173.
[13] G. Bevelander and H. Nakahara // *Calcif. Tissue Res*. **3** (1969) 84.
[14] K. Wada // *Biomineralisation* **6** (1972) 141.
[15] H. Mutvei // *Scanning Electron Microsc*. **2** (1979) 457.
[16] S. Manne, C. M. Zaremba, R. Giles, L. Huggins, D. A. Walters, A. M. Belcher, D. E. Morse, G. D. Stucky, J. M. Didymus, S. Mann and P. K. Hansma // *Proc. R. Soc. Lond. B Biol. Sci.* **256** (1994) 17.
[17] T. E. Schaffer, C. Ionescu-Zanetti, R. Proksch, M. Fritz, D. A. Walters, N. Almqvist, C. M. Zaremba, A. M. Belcher, B. L. Smith, G. D. Stucky, D. E. Morse and P.K. Hansma // *Chemistry of Materials* **9** (1997) 1731.
[18] D. R. Katti and K. S. Katti // *Journal of Materials Science* **36** (2001) 1411.
[19] D.R. Katti, K.S. Katti, J. Tang and M. Sarikaya, In: *Proc 15th ASCE Engineering Mechanics Conference*, ed. by A. Smyth (New York, 2002).
[20] D.R. Katti, K.S. Katti, J. Sopp and M. Sarikaya // *Journal of Computational and Theoretical Polymer Science* **11** (2001) 397.
[21] R.Z. Wang, Z. Suo, A.G. Evans, N. Yao and I.A. Aksay // *J. Mater. Res.* **16** (2001) 2485.
[22] A.G. Evans, Z. Suo, R.Z. Wang, I.A Aksay, M.Y. He and J.W. Huchinson // *J. Mater. Res*. **16** (2001) 2475.
[23] P.Ghosh, D. R. Katti and K.S. Katti, In: *Proc. 17th ASCE Engineering Mechanics Conference*, ed. by H. Sheldon (Delaware, 2004).